[Papers in Palaeontology, Vol. 11, Part 4, 2025, e70026]

Recovering lost time in Syria: a new Eocene stereogenyin turtle from the Aleppo Plateau

by WAFA A. ALHALABI[1,*], DONATO J. MARTUCCI NETO[1], GABRIEL S. FERREIRA[2,3], ISSAM BOU JAOUDE[4], HASSAN M. NASER[5], JOULIANA AYOUB[6], LAMA ABBOUD[6], RIM SHATI[6], EDUARDO A. M. KOUTSOUKOS[7] *and* MAX C. LANGER[1]

[1]Derpartamento de Biologia, FFCLRP, Universidade de São Paulo, Av. Bandeirantes 3900, 14.040-901 Ribeirão Preto, SP, Brazil; wafaadelalhalabi@gmail.com
[2]Senckenberg Centre for Human Evolution and Palaeoenvironment at the University of Tübingen, Hölderlinstrasse 12, 72074 Tübingen, Germany
[3]Department of Geosciences, Eberhard Karls University of Tübingen, Hölderlinstrasse 12, 72074 Tübingen, Germany
[4]Morrison Hershfield, 2932 Baseline Rd, Ottawa, ON K2H 1B1, Canada
[5]General Establishment for Geology and Mineral Resources in Homs, Syria
[6]General Establishment for Geology and Mineral Resources in Damascus, Syria
[7]Institut für Geowissenschaften, Universität Heidelberg, Im Neuenheimer Feld 234, 69120 Heidelberg, Germany
*Corresponding author

Typescript received 6 March 2025; accepted in revised form 7 June 2025

Abstract: Across the Arabian Platform, fossil turtles have been recovered from deposits dating back to the Cretaceous. In Syria, such remains are mostly fragmentary, recovered from the phosphatic deposits around Palmyra, as well as from the Pleistocene Nadaouiyeh Aïn Askar archaeological site. Here we report a new genus and species, *Syriemys lelunensis*, represented by a fully preserved inner cast of the shell, plus some plastral, pelvic and hind-limb bones, some enclosed within the cast. The specimen was collected from the Al-Zarefeh Quarry, near Afrin, in Aleppo Governorate, with foraminifera extracted from the surrounding rock indicating an early Eocene age. *Syriemys lelunensis* can be ascribed to the pleurodiran clade Stereogenyini based on a short cranial lobe of the plastron, which does not extend beyond the cranial margin of the carapace, a short epiplastral symphysis, and very reduced gular, extragular and humeral scutes. *Syriemys lelunensis* also differs from all other known members of the group that have a preserved shell by the presence of three autapomorphic traits: seven neural bones extending at least to costal bone 7, a nuchal bone with a cranial edge half the lateromedial breadth of its widest part, and a shallow anal notch formed by short xiphiplastral processes. This discovery pushes the origin of Stereogenyini back at least to the early Eocene, providing further support for a Mediterranean ancestral geographical range for the group. Finally, *Sy. lelunensis* represents the first new species of extinct vertebrate ever described from Syria.

Key words: Syria, Stereogenyini, *Syriemys lelunensis*, Eocene.

STEREOGENYINI represent an extinct group of pleurodire turtles with a coastal or marine lifestyle (Ferreira *et al.* 2015, 2018a). Known from the Eocene–Miocene of the Mediterranean realm (e.g. *Cordichelys antiqua*, *Latentemys plowdeni*, *Lemurchelys diasphax*, *Mogharemys blackenhorni* and *Stereogenys cromeri*; Andrews 1901, 1903; Dacqué 1912; Gaffney *et al.* 2011), the Caribbean area (e.g. '*Bairdemys*' *healeyorum*, *Bairdemys* spp.; Wood & Díaz de Gamero 1971; Gaffney & Wood 2002; Gaffney *et al.* 2008; Weems & Knight 2013; Ferreira *et al.* 2015), and the northern Indian Ocean (e.g. *Brontochelys gaffneyi*, *Piramys auffenbergi* and *Shweboemys pilgrimi*; Swinton 1939; Wood 1970; Prasad 1974), their records suggest a northern tropical distribution during most of the Cenozoic and an extinction around the Miocene–Pliocene boundary. Here, we describe a new Stereogenyini species, from Eocene deposits of northern Syria, which corresponds to the oldest confirmed record of that group. In fact, Stereogenyini represent the only podocnemidids previously reported from the Arabian Plate, with *Shweboemys* tentatively recorded in Miocene deposits of Oman (Roger *et al.* 1994) and Saudi Arabia (Thomas 1982), and *Stereogenys* in the Oligocene of the former country (Thomas *et al.* 1989).

The new fossil was discovered in 2010, at the Al-Zarefeh Quarry in the Aleppo Governorate (Fig. 1A), among the debris following a controlled explosion to break up large limestone blocks for processing. The specimen was found in two pieces and brought to the attention of the quarry owner, Mr Muhammad Al-Ibrahim. Recognizing its potential significance, he transferred the fossil to the General Establishment for Geology and Mineral Resources (GEGMR) office in Aleppo, where it

doi: 10.1002/spp2.70026

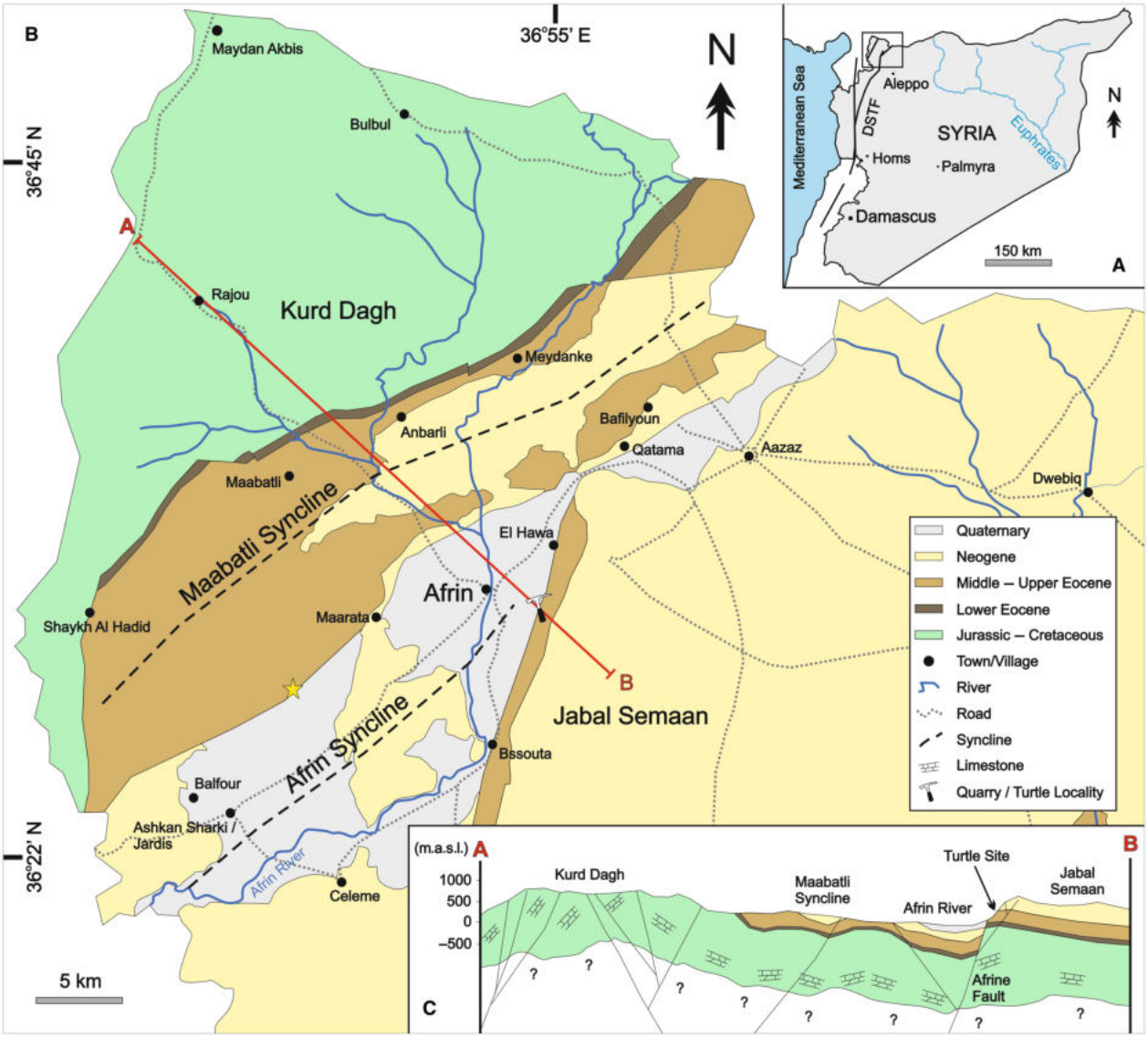

FIG. 1. A, map of Syria highlighting the location of the study area (boxed area). B, surface exposure of rocks in the study area: the yellow star indicates the location of the lithological log in Figure 2, and the line 'A–B' indicates the cross-sectional profile in C, highlighting the deposits and structural setting of the area (modified from Protasevich *et al.* 1963). *Abbreviation*: DSTF, Dead Sea transform fault.

was received by the former GEGMR director, Mr Abdo Alwan, examined by geologists Muhammad Ibrahim, Ali Abdullah, Abdo Alwan and Muhammad Shaib, and subsequently put on display. By 2023, geologist Hassan Naser informed the first author about the fossil; the GEGMR office in Damascus was contacted and arrangements were made to transfer the specimen to that institution, where it was officially catalogued.

Fossil turtles have been previously documented in Syria from the Cretaceous phosphatic deposits of the Palmyra area. These include fragmentary remains of marine or coastal cryptodires (Chelonioidea) and pleurodires (Bothremydidae), the latter possibly including representatives of the Taphrosphyini (Bardet *et al.* 2000; Al Maleh & Bardet 2003). Furthermore, the Pleistocene deposits of the Nadaouiyeh Aïn Askar archaeological site include remains likely to represent emydid cryptodirans (Savioz & Morel 2005). The new material described here represents not only the first well-diagnosed fossil turtle from Syria, but also the first new species of an extinct vertebrate described for the country.

This is the second contribution to a series of papers, started with Alhalabi *et al.* (2024), entitled 'Recovering Lost Time in Syria'. Future publications of this series are currently in preparation and will continue to explore the vertebrate fossils of the country.

GEOLOGICAL SETTING & AGE

The limestone quarry that yielded the new turtle is located in northern Syria, close to the border with Turkey (Fig. 1A), and supplies coarse aggregates for the area. It is located on the western slopes of Mount Semaan, at an elevation of *c.* 360 m.a.s.l. The slope extends in a NE–SW direction, overlooking the Afrin plain at an elevation of *c.* 300–550 m.a.s.l. The Afrin plain itself, where Afrin village is located, is positioned between Mount Semaan and the Maabatli syncline, at an elevation of 250–300 m.a.s.l. All of these topographic features are structurally controlled by the Dead Sea transform fault (DSTF; Fig. 1). The DSTF is an active transform boundary between the Arabian and the Levantine plates (Brew *et al.* 2002). The Afrin plain, which is a pull apart basin, and the slope where the quarry is located are on the active branch of the DSTF (Rukieh *et al.* 2005).

The Afrin district is mainly covered by deposits of Jurassic–Cretaceous age in its northwesternmost part (Kurd Dagh mountains) and by deposits of Eocene and Miocene age at its southeastern part, the Maabatli syncline and Mount Semaan (Fig. 1B). The Kurd Dagh mountains and the Maabatli syncline are separated by outcrops of an argillaceous limestone, which was ascribed to the lower Eocene (Protasevich *et al.* 1963). Close to Ashkan Sharki, this argillaceous limestone is covered by a hard grey to white nummulitic limestone and by a light grey argillaceous limestone, ascribed to the middle and upper Eocene, respectively (Figs 1B, 2), all of which was deposited in shallow waters (Brew *et al.* 2002). The lower Eocene limestone also includes some tuffs (Protasevich *et al.* 1966) but this is barely exposed in the eastern part of the Maabatli syncline and the western slope of Mount Semaan. The lithology that preserved the fossil turtle is mainly composed of hard grey to white limestone, with pinkish veins, which is also ubiquitous in the quarry exposures and better fits the middle Eocene limestone of Brew *et al.* (2002). However, based on the geological map and cross-sectional profile, the turtle site appears to be somewhat higher in the stratigraphy (Fig. 1).

Rock samples extracted from around the turtle shell cast provided a foraminiferal record that enabled correlation of the fossil-bearing deposits with the Berggren *et al.* (1995) and Berggren & Pearson (2005) biozones. Confirmed taxa include *Acarinina angulosa*, *Ac. soldadoensis*, *Subbotina eocaena* and *Parasubbotina inaequispira*, whereas *Ac. pseudotopilensis*, *Chiloguembelina* sp., *Morozovella aragonensis*, *Mor. lensiformis*, *Mor. velacoensis*, *Su. linaperta* and *Su. velascoensis*, are also likely to be present. This suggests a correlation to the lowest Eocene (56–54.4 Ma), that is the uppermost part of Zone P5 of Berggren *et al.* (1995) (Berggren & Pearson 2005).

MATERIAL & METHOD

GEGMRD 0002 is permanently housed at the General Establishment for Geology and Mineral Resources in Damascus (GEGMRD). The GEGMRD was established in 1977 under official government decree no. 136, as an official institution operating under the Ministry of Petroleum and Mineral Resources. Given that Syria currently lacks a natural history museum or official palaeontological collection, an agreement was made to store all fossils collected in the country at the GEGMRD.

Measurements were taken using a digital calliper accurate to 0.01 mm. The specimen was scanned using a Philips medical computed tomography (CT) scanner at Daffodil 88 Medical Centre, a private facility in Damascus. The specimen was scanned with the voltage set to 120 kV, the current to 263 μA, and the voxel size to 0.8535 mm. Three-dimensional segmentation and visualization were conducted using Amira v2022.2 (Thermo Fisher Scientific). Rock samples were collected from the turtle shell cast, soaked in water for 24 h, and washed to remove marl and clay residues. The cleaned samples were then oven-dried for 1 min and analysed using a Nikon microscope.

The nomenclature for the turtle shell bones and scutes follows Hutchison & Bramble (1981). We use the International Committee on Veterinary Gross Anatomical Nomenclature (ICVGAN 2005) to describe the body parts of GEGMRD 0002, with the propodium oriented lateromedially on the horizontal plane (Romer 1956). Hence, the major trochanter expands cranially from the proximal portion of the femur.

The phylogenetic analysis was conducted by adding GEGMRD 0002 to the character–taxon matrix of Ferreira *et al.* (2024) (Appendix S1; Alhalabi *et al.* 2025). Because some characters incorporate errors introduced by the use of synonymous terminology for the gulars/extragulars and intergular/gular scutes, we further modified that matrix by adjusting the statements and scorings for characters 230, 233, 234 and 242 (Appendix S2). Also, some scorings of *Stupendemys geographica* were updated (Appendix S2) based on recently discovered specimens (Cadena *et al.* 2020, 2021). All characters were treated with the same weight, and some were ordered (as in the previous analysis of Ferreira *et al.* 2024). The new matrix was analysed in TNT v1.6 with traditional search, using the tree-bisection reconnection (TBR) swapping algorithm, with 1000 replicates holding 20 trees, and random seed = 1. A second round of TBR was conducted on the saved trees and a strict consensus was calculated to summarize the results.

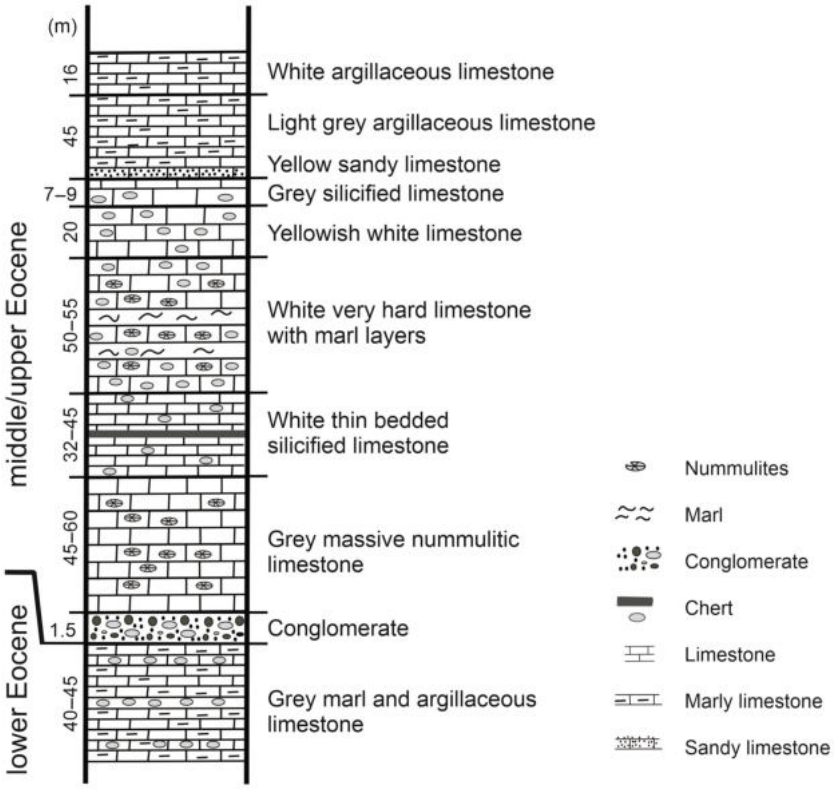

FIG. 2. Lithological log near Ashkan Sharki Village (yellow star in Fig. 1B), showing putative lower–upper Eocene deposits (based on data from Protasevich *et al.* 1966).

Palaeogeographical maps were created using the packages terra (Hijmans 2025), sf (v1.0-21; Pebesma 2018; Pebesma & Bivand 2023), and rgplates (v0.6.0; Müller *et al.* 2018; Kocsis *et al.* 2024) in R (R Core Team 2024) modifying a script created by Ádám T. Kocsis (available at https://gplates.github.io/rgplates). We used data from Kocsis & Scotese (2021) to present the contours and position of the possible landmasses at 50, 35, 20 and 10 Ma, and a proxy-corrected HadCM3L climate model to plot the mean annual air surface temperatures (Scotese *et al.* 2021, after Valdes *et al.* 2021) for those same time slices.

SYSTEMATIC PALAEONTOLOGY

PLEURODIRA Cope 1865
PELOMEDUSOIDES de Broin 1988
PODOCNEMIDIDAE Cope 1868
STEREOGENYINI Gaffney *et al.* 2011
Genus *Syriemys* nov.
Figures 3–6

LSID. https://zoobank.org/NomenclaturalActs/d2eff823-40ea-4efb-adf5-b4837df56467

Derivation of name. The genus name joins the Greek words Συρία (*Suría*) and ἐμύς (*emús*), latinized as 'Syria' and 'emys', respectively, for 'Syria' and 'turtle'.

Type species. Syriemys lelunensis.

Diagnosis. As for type and only species.

Syriemys lelunensis sp. nov.

LSID. https://zoobank.org/NomenclaturalActs/d34a111c-cbbb-413a-8282-a39e7f1017f1/

Derivation of name. The species epithet derives from the Kurdish name (*Lelun*) of the highland area where the fossil was found, also known as Mount Semaan. 'Lelun' may refer to the olive fruit before ripening (*LeLun*), meaning 'excessive bitterness', or stem from *LeyLan*, which denotes a mirage. Another possible origin is *Lulan*, meaning 'twisting' or 'crescent-shaped', a characteristic that aligns with the mountain's crescent-like form on its western end (Barakat 2006).

Holotype. GEGMRD 0002 (Figs 3–6) is mainly composed of an internal shell cast, but also includes parts of the entoplastron, the right hyoplastron, and both epi-, hypo- and xiphiplastra.

The right and left pelvic bones and the femora were preserved inside the cast.

Type locality & horizon. The Al-Zarefeh Quarry is an extraction site of limestone gravel used for construction managed by the GEGMR office in Aleppo. The quarry is located *c.* 3.5 km east of Afrin (Efrin) in the Aleppo Governorate, on the western edge of Lelun Mountain. Coordinates: 36°29′31″N, 36°54′04″E. The hard grey to white limestone that is ubiquitous in the quarry and in which the fossil turtle was preserved, matches the middle Eocene deposits described for the area by Brew *et al.* (2002). However, the foraminifera extracted from around the turtle shell cast indicate an early Eocene age.

Diagnosis. Syriemys lelunensis can be ascribed to Pleurodira by the suture of the pelvic girdle to the shell, to Pelomedusoides by possessing a pair of small, rounded and laterally placed mesoplastra, and to Stereogenyini by the presence of a short and rounded cranial plastral lobe that does not extend beyond the cranial margin of the carapace, a short epiplastral symphysis, and very reduced gular, extragular and humeral scutes. It differs from '*Ba.*' *healeyorum* and *Ba. venezuelensis* by the presence of a nuchal notch and axillary buttresses that reach peripheral bones 2. It differs from *Co. antiqua* by bearing a shallower nuchal notch, a pectoral scute that extends over two-thirds of the entoplastron, and very small extragular scutes that do not reach the entoplastron (as in '*Ba.*' *healeyorum*, but unknown in *Ba. venezuelensis*). Finally, it differs from all other Stereogenyini that have a preserved shell by the presence of seven neural bones extending at least to costal bone 7, a nuchal bone with a cranial edge half the lateromedial breadth of its widest part, and a shallower anal notch formed by shorter xiphiplastral processes.

Description. The carapace morphology (Figs 3, 4) is preserved only as impressions of the sutures in the internal cast, showing the contact between all of the bones. The carapace is 53 cm long at the midline and 44 mm wide at the level of costal bones 4; these are linear measurements, not following the convexity of the carapace. It is oval shaped, slightly tapering caudally. The nuchal bone is trapezoidal, *c.* 30% wider than long, with a rounded caudal margin that is almost twice as broad as the cranial edge, contacting peripheral bones 1 laterally, and both neural bone 1 and costal bones 1 caudally. It should be highlighted that the dorsal shape of the carapacial bones may differ from the morphology they assume on the visceral side of the carapace. The following descriptions are based on what is preserved (i.e. the cast of the visceral carapacial surface) and should thus be taken with caution. The neural series comprises seven bones, all twice as long as wide, except for the sixth element, which is only slightly longer than wide. Neural bones 1–6 are wider cranially than caudally, but the condition in the seventh element is unclear. The shape of the first neural bone seems to be different from that of the other bones in the series, it contacts the nuchal bone cranially, the first costal bones laterally, and neural bone 2 caudally. Thus, its dorsal surface would most likely have had a rectangular outline. Neural bone 3 is the

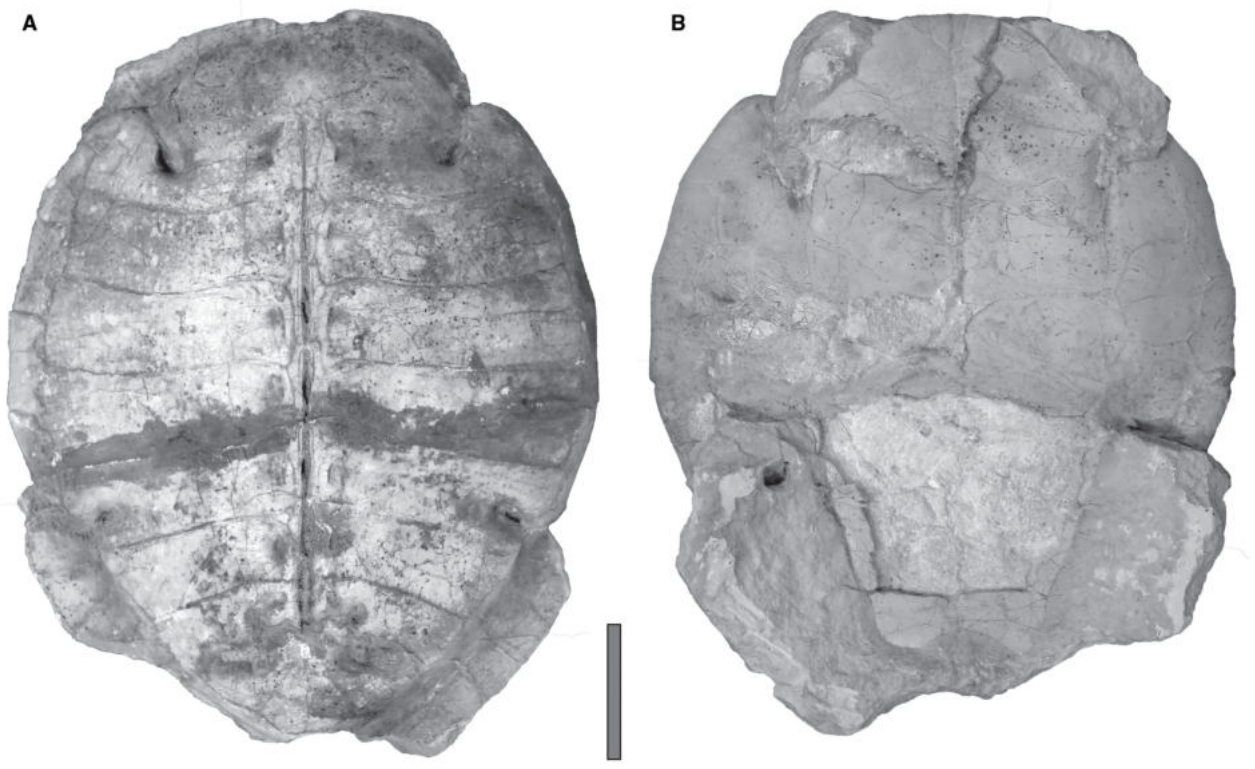

FIG. 3. *Syriemys lelunensis* gen. et sp. nov. (GEGMRD 0002), early Eocene of Syria. Photographs of the inner cast of the shell showing aspects of the carapace and plastron anatomy in: A, dorsal; B, ventral view. Scale bar represents 10 cm.

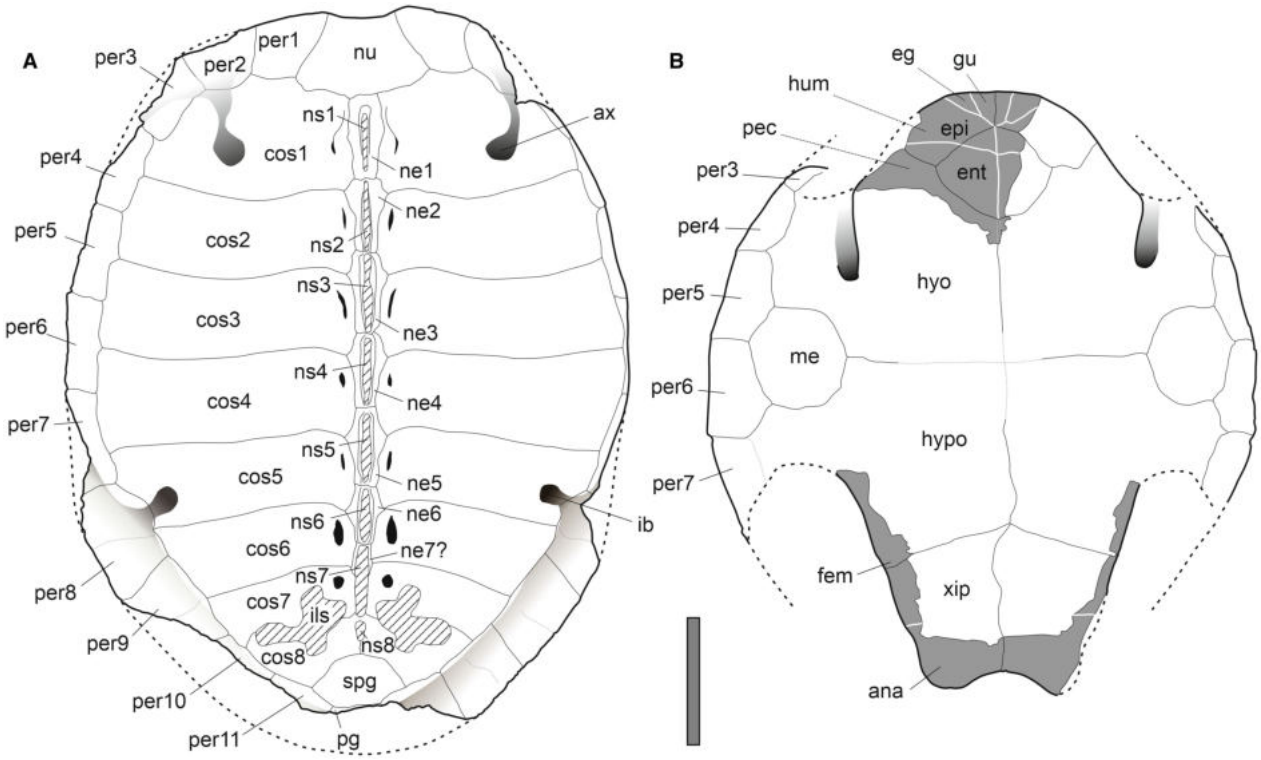

FIG. 4. *Syriemys lelunensis* gen. et sp. nov. (GEGMRD 0002), early Eocene of Syria. Drawings of the inner cast of: A, carapace; B, plastron. *Abbreviations*: ana, anal scute; ax, axillary buttress; cos1–8, costal bones 1–8; eg, extragular scute; ent, entoplastron; epi, epiplastron; fem, femoral scute; gu, gular scute; hum, humeral scute; hyo, hyoplastron; hypo, hypoplastron; ib, inguinal buttress; ils, iliac scar; me, mesoplastron; ne1–7, neural bones 1–7; nu, nuchal bone; pec, pectoral scute; per1–11, peripheral bones 1–11; pg, pygal bone; spg, suprapygal bone; ns1–8, neural spine scars 1–8; xip, xiphiplastron. Dashed lines indicate reconstructed contour of the shell; grey shadowing indicates holes in the cast corresponding to the shell buttresses; dotted lines on peripheral plates 8–10 represent sulci left by the marginal scutes on the visceral surface of the carapace; hatched areas in A indicate iliac and vertebral articulations; preserved bones in B are shown in dark grey. Scale bar represents 10 cm.

longest and 2 the widest of the series. Neural bone 2 contacts costal bones 1 craniolaterally, costal bones 2 laterally, and neural bone 3 caudally. Neural bones 3–6 follow the same pattern as neural bone 2: neural bone 3 contacts costal bones 2 craniolaterally and costal bones 3 laterally; neural bone 4 contacts costal bones 3 craniolaterally and costal bones 4 laterally; neural bone 5 contacts costal bones 4 craniolaterally and costal bones 5 laterally; and neural bone 6 contacts costal bones 5 craniolaterally, costal bones 6 laterally, and probably neural bone 7 caudally. The neural series is relatively long, extending at least to costal bones 7, but most probably not reaching costal bones 8. The suprapygal bone is trapezoidal, slightly wider than long, and with a rounded cranial margin. Only a small portion of the cast of the pygal bone is preserved, showing its contacts with the suprapygal bone cranially and with both peripheral bones 11 laterally.

The first costal bone is the longest, the fourth is the widest, whereas the eighth is the smallest in all dimensions and the only one in the series that clearly contacts its counterpart medially, although this was probably also the case for costal bones 7 and 8. Regarding their contacts, costal bone 1 contacts the nuchal and peripheral bones 1 and 2 cranially, peripheral bones 3 and 4 laterally, and costal bone 2 caudally. Costal bones 2–5 follow a similar pattern, each contacting the two adjacent peripheral bones laterally: costal bone 2 contacts peripheral bones 4 and 5; costal bone 3, peripheral bones 5 and 6; costal bone 4, peripheral bones 6 and 7; and costal bone 5, peripheral bones 7 and 8. Costal bone 6 contacts its counterpart medially and peripheral bones 8 and 9 laterally. Costal bones 7 and 8 probably contact their counterparts medially, costal bone 7 contacts peripheral bones 9 and 10 laterally, whereas costal bone 8 contacts peripheral bones 10 and 11 laterally and the suprapygal bone caudally. The scars left by the first two thoracic ribs are relatively robust, but the costovertebral tunnel seems very shallow. The axillary scar is restricted to the first costal bones, but is relatively short, extending in a caudomedial to craniolateral direction for less than half of the total length of the bone. Costal bones 5 bear the inguinal scar, which is very reduced, restricted to its lateral edge. The iliac scar has a triradiate shape and lies over costal bones 7 and 8, not reaching the suprapygal element. Peripheral bone 1 is almost two-thirds wider cranially than caudally and the other peripherals are more consistent in these measurements. Peripheral bones 3–10 are longer than wide, with the opposite being the case for peripheral bones 1 and 2, whereas the 11th elements

are not entirely preserved. The axillary scar extends craniolaterally to peripheral bones 2 and 3, whereas the inguinal scar reaches peripheral bone 8. Peripheral bones 8–10 preserve the sulci left by the marginal scutes on the visceral surface of the shell, which lie at the mid-length of the bones and match the sutures between subsequent costal bones.

The plastron consists of 11 bones (Figs 3, 4): the entoplastron and paired epiplastra, hyoplastra, hypoplastra, mesoplastra and xiphiplastra. Only parts of both epiplastra, the entoplastron, the right hyoplastron, and both hypo- and xiphiplastra are preserved, but the contact between all plastral bones can be observed in the internal cast. The plastron is 46 cm long (measured at the midline, from the cranial margin of the plastron to the cranial margin of the anal notch) and 38 cm wide (between the lateral edges of the mesoplastra). The cranial lobe is short, about half the length of the caudal lobe. The entoplastron has a rhomboidal shape and is slightly wider than long, contacting the epiplastron craniolaterally and the hyoplastron caudolaterally. The epiplastra are large (about the size of the entoplastron), and they contact the counterpart craniomedially, the entoplastron caudomedially and the hyoplastron caudolaterally. The hyoplastron has the largest maximum length of the plastral bones and forms the cranial portion of the bridge, laterally contacting peripheral bones 2–5. The mesoplastron is rounded and lateral, only slightly larger than the entoplastron. It lies between the hyo- and hypoplastra and laterally contacts peripheral bones 5 and 6, forming the middle portion of the bridge. The hypoplastron has the longest midline length of the plastral bones and forms the caudal portion of the bridge, laterally contacting peripheral bones 6 and 7. The xiphiplastron is relatively large, as long at the midline as the hyoplastron. Its lateral margin is straight, lacking the constriction caused by the femoroanal sulcus. The caudal processes are short and rounded, forming a shallow and wide anal notch.

Some sulci between the scutes are visible in the preserved bone plates of the plastron. The gular scute is short and trapezoidal; it reaches the cranial margin of the plastron but does not extend over the entoplastron. It contacts the extragular scutes laterally and the humeral scutes caudally, completely separating the extragular scutes from one another. The extragular scutes are very small and triangular, reaching the cranial edge of the plastron. They are restricted to the epiplastron and are located between the gular and humeral scutes. The humeral scutes are twice as large as the gular and extragular scutes combined. They overlay the epiplastra and entoplastron but do not reach the hyoplastra caudally, or reach them only slightly laterally. Aside from the previously mentioned contacts, the humeropectoral sulci extend lateromedially from the epi- to the entoplastron, with the humeral scutes covering only the cranial third of the entoplastron. Only the cranialmost portion of the pectoral scutes is visible. They are larger than the other scutes, overlaying two-thirds of the entoplastron, the caudal corner of the epiplastron, and the entire preserved portion of the hyoplastron. On each xiphiplastra, a small lateral portion of the femoroanal sulcus is visible, located at about half the length of the bone.

Both the pelvic girdle and the femora were preserved inside the shell cast and could be reconstructed using the CT data (Figs 5, 6). The pelvic bones were displaced from their original position but are nearly complete, with the three bones being almost the same size. The ilium is considerably flattened lateromedially and its dorsalmost part is not preserved. The ventral surface is expanded to articulate with the pubis and ischium, forming the dorsal part of the acetabulum. In the ventral part of that structure, the pubis articulates caudally with the ischium. The epipubic process is very thin and projects craniomedially. The surface of the pubis that articulates with the xiphiplastron is slightly deformed, but shows a broad roughly triangular sutural contact. The ischium articular surface for the xiphiplastron could not be reconstructed with accuracy, but it is roughly oval shaped, with the long axis oriented caudolaterally to craniomedially. The ischium and pubis form a broad thyroid fenestra ventral to the acetabulum, which is oval and slightly elongated cranioventrally to caudodorsally.

The left femur is well-preserved and lies near the pelvic girdle, with its proximal end near, but not articulated with, the acetabulum. The right femur is rotated, displaced cranially and more deformed than the left one. The femora are *c.* 10 cm long, with a largely sigmoid shape in cranial/caudal views, although the shaft is straight. The femoral head is large and well-projected from the shaft, with the articular surface tilted *c.* 33° relative to the shaft axis (measured from the midline of the shaft in relation to the inclination of the articular surface, with the inflection point located at the proximal edge of the articular surface). The two trochanters are parallel to one another, forming a wide and shallow intertrochanteric fossa. The major trochanter is only slightly larger than the minor trochanter and projects craniodorsally, whereas the minor trochanter projects caudoventrally. The trochanters are separated from the femoral head by shallow but distinctive notches and expand distal to the femoral head. The distal end of the bone is curved ventrally, showing a clear distinction between the fibular condyle, which is more prominent, and the tibial condyle. The condyles are separated by a well-developed intercondylar fossa.

PHYLOGENETIC RESULTS

The phylogenetic analysis of the modified matrix after the inclusion of *Sy. lelunensis* resulted in 1728 trees of 527 steps. Their strict consensus (Fig. 7) is well-resolved and like that of other studies based on previous versions of that data-matrix (Ferreira *et al.* 2024). The newly added *Sy. lelunensis* is well set within the Stereogenyini and Stereogenyina clades (*sensu* Ferreira *et al.* 2015) as sister to *Co. antiqua* (i.e. external to the Stereogenyita/Bairdemydita dichotomy; Ferreira *et al.* 2018a, 2018b). That sister taxon relation is supported by three synapomorphies: an embayed nuchal bone (char. 170, state 1), an axillary buttress that reaches peripheral bone 2 (char. 193, state 0), and a dorsoventrally flattened shell (char. 206, state 1). The clades Stereogenyini and Stereogenyina are well supported, both of them by seven synapomorphies. The monophyly of Stereogenyini is supported by characters 25, 26, 71, 74, 79, 81 and 111, whereas that of

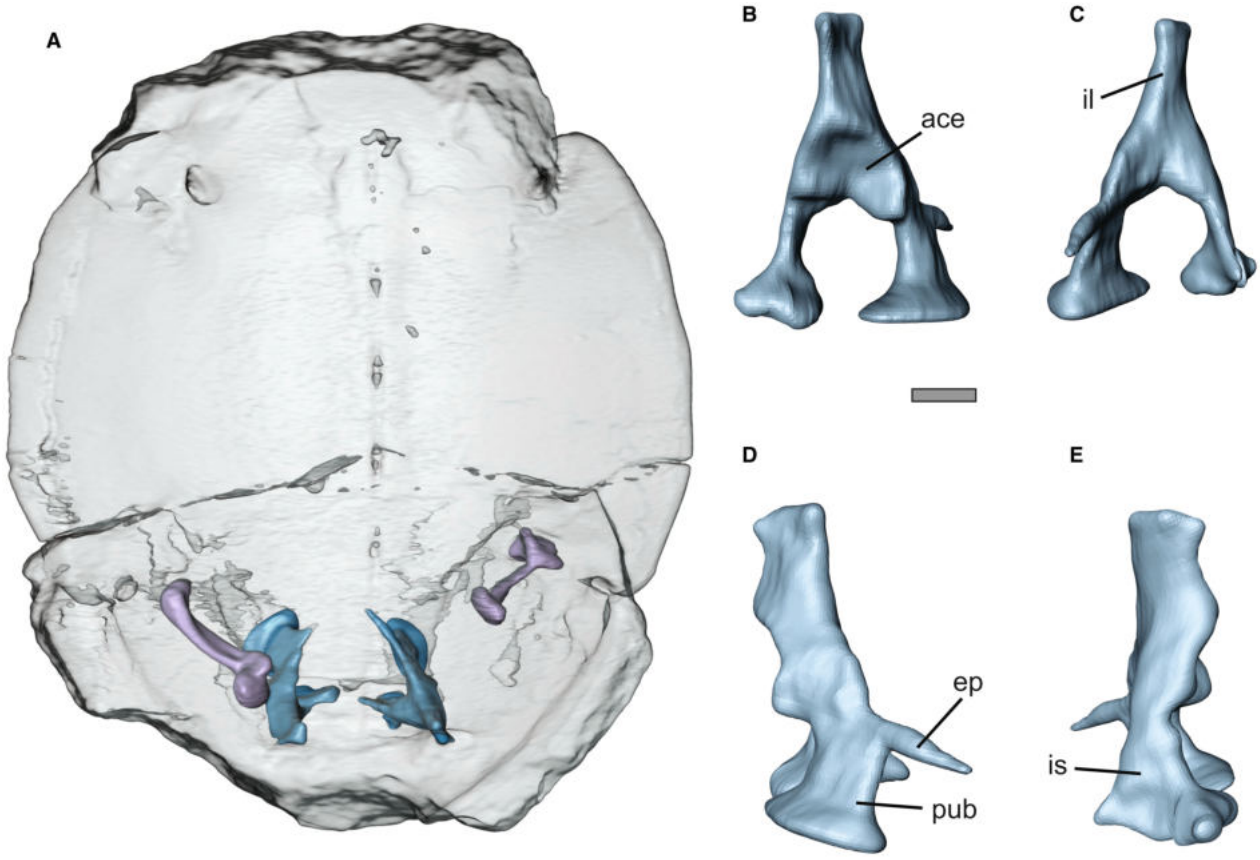

FIG. 5. *Syriemys lelunensis* gen. et sp. nov. (GEGMRD 0002), early Eocene of Syria. CT rendered images. A, dorsal view of the shell cast with pelvic bones and femora in their preserved positions. B–E, right pelvic bones in: B, lateral; C, medial; D, cranial; E, caudal view. *Abbreviations*: ace, acetabulum; ep, epipubic process; il, ilium; is, ischium; pub, pubis. Scale bar represents 2 cm (B–E).

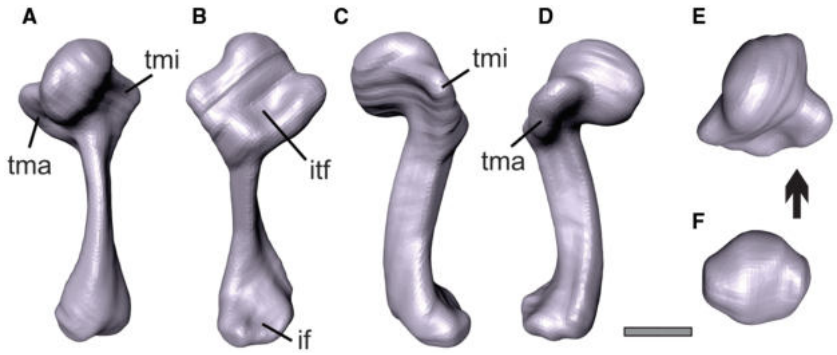

FIG. 6. *Syriemys lelunensis* gen. et sp. nov. (GEGMRD 0002), early Eocene of Syria. CT rendered images of the left femur in: A, dorsal; B, ventral; C, caudal; D, cranial; E, proximal; F, distal view. *Abbreviations*: if, intercondylar fossa; itf, intertrochanteric fossa; tma, major trochanter; tmi, minor trochanter. Arrow in E–F points dorsally. Scale bar represents 2 cm.

Stereogenyina is based on characters 55, 56, 70, 75, 76, 90 and 128. All of the characters are, nevertheless, related to the skulls: for example, very small to absent fossae precolumellaris (char. 80, state 0) for the former or the presence of a secondary palate (char. 75, state 1) for the latter.

DISCUSSION

Even though most Stereogenyini are known exclusively from cranial remains, those with preserved shells (i.e. *Co. antiqua*, '*Ba.*' *healeyorum* and *Ba. venezuelensis*) show many similarities to *Sy. lelunensis*. Its relatively short

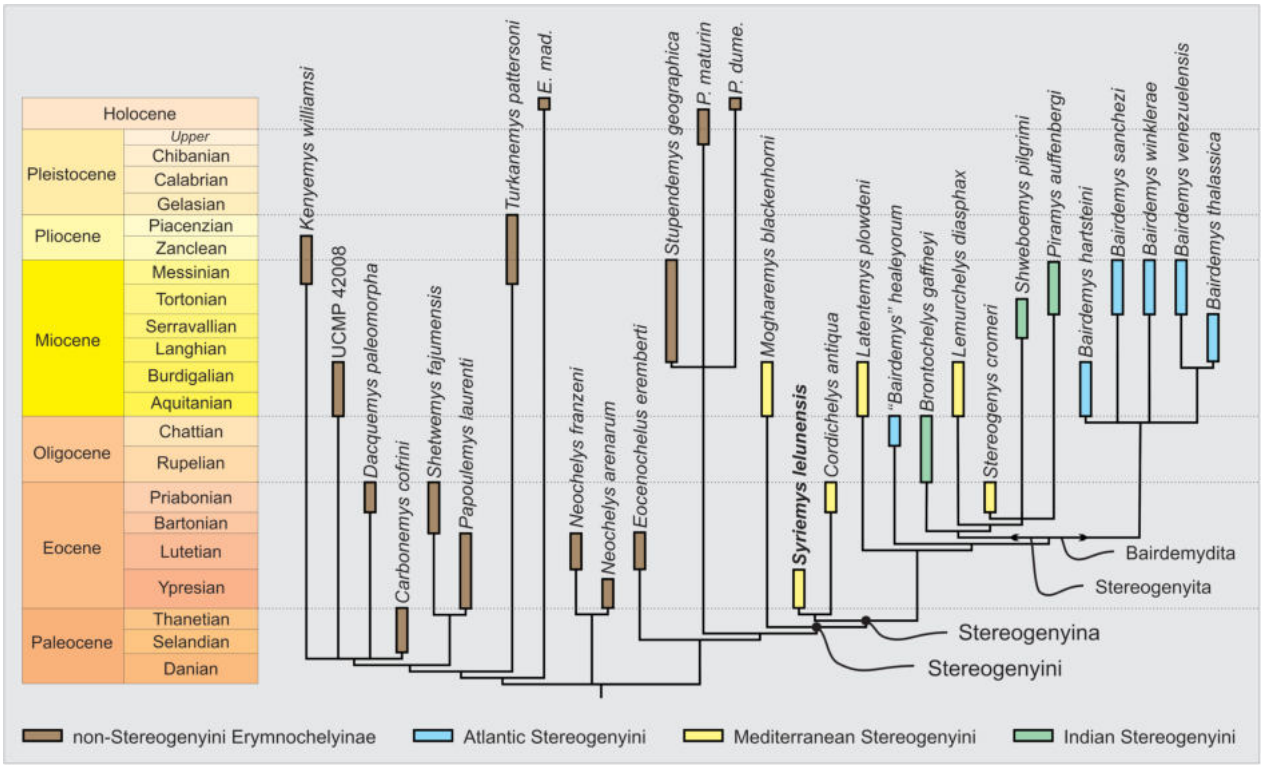

FIG. 7. Excerpt of the strict consensus of 1728 most parsimonious trees in the present phylogenetic analysis, showing the position of *Syriemys lelunensis* in Erymnochelyinae. Terminals scaled to the Cenozoic timescale (Cohen *et al.* 2013; v2024/12). Arrow, stem-based clade; black circle, node-based clade. *Abbreviations*: *dume.*, *dumerilianus*; *E.*, *Erymnochelys*; *mad.*, *madagascariensis*; *P.*, *Peltocephalus*; UCMP, University of California Museum of Paleontology.

plastron, with a very short and round cranial lobe that does not extend beyond the cranial line of the carapace, and short epiplastral symphysis, are typical traits of the Stereogenyini plastron (Wood & Díaz de Gamero 1971; Weems & Knight 2013; Cherney *et al.* 2020). Among Stereogenyini, *Sy. lelunensis* shows many similarities to '*Ba.*' *healeyorum*, such as very reduced extragular scutes, restricted to the epiplastra, and pectoral scutes that extend more cranially, overlaying two-thirds of the entoplastron. It also shares traits with *Co. antiqua*, as shown by the phylogenetic results. Most importantly, it can be distinguished from all other Stereogenyini by the presence of three autapomorphic characters: a shallow anal notch formed by shorter xiphiplastral processes, a nuchal bone with a lateromedially narrow cranial edge (half its maximum width), and seven neural bones that extend to costal bone 7. Most non-Stereogenyini erymnochelyines have a neural series composed of only six bones, except for *Papoulemys laurenti* and some *Neochelys* species (e.g. *Ne. capellini*, *Ne. salmanticensis* and *Ne. zamorensis*; de Broin 1977; Pérez-García *et al.* 2023, 2024) in which seven (sometimes eight; Pérez-García *et al.* 2024) bones are present. Among Stereogenyini the neural series is more variable. Whereas *Co. antiqua* and '*Ba.*' *healeyorum* have the common count of six neural bones (Gaffney *et al.* 2011; Weems & Knight 2013; Cherney *et al.* 2020), *Ba. venezuelensis* completely lacks those elements (Wood & Díaz de Gamero 1971) and *Andrewsemys libyca* (originally assigned to *Stereogenys*, but currently with unclear affinities to Stereogenyini; Pérez-García *et al.* 2017) has a series of eight neural bones, although lacking neural bone 1. Finally, the femur of *Sy. lelunensis* has a slenderer shaft and a more curved distal condyle, compared with '*Ba.*' *healeyorum* (Weems & Knight 2013), which is the only other Stereogenyini with a known femur. Thus, *Sy. lelunensis* can be confidently recognized as a new genus and species of that group.

Previously, the oldest confirmed records of Stereogenyini (i.e. *Ste. cromeri* and *Co. antiqua*) came from the late Eocene (Priabonian) of Egypt (Kampouridis *et al.* 2023). The discovery of *Sy. lelunensis* pushes the origin of the group back minimally into the early Eocene, approaching the oldest records of other Erymnochelyinae (e.g. *Carbonemys cofrini*, Paleocene of Colombia). It also provides extra support for a Mediterranean (i.e. north Africa and west Arabia) ancestral geographical range for Stereogenyini, as already suggested by the Egyptian provenance of its earliest branching members (Fig. 7) and a

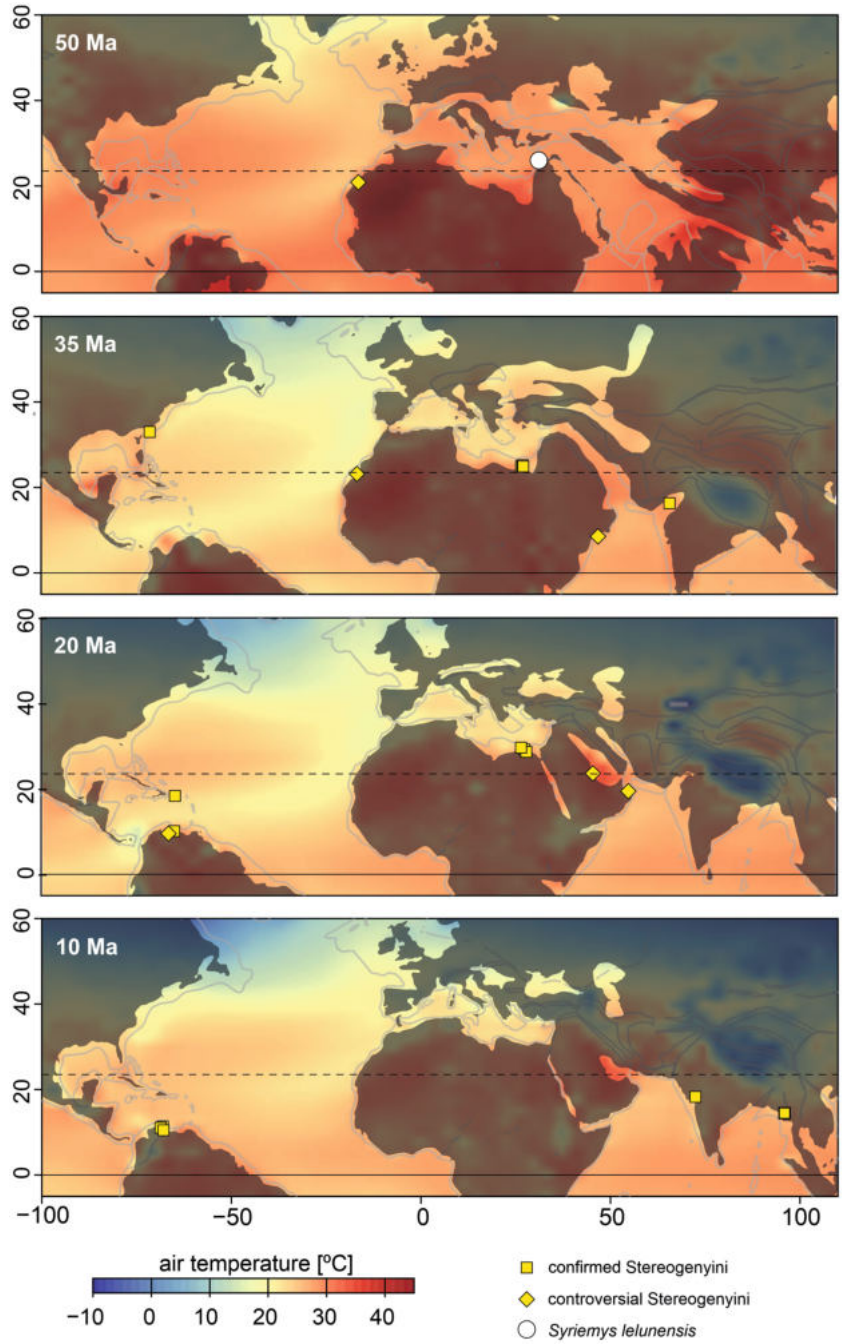

FIG. 8. Palaeogeographic maps (produced as detailed in the Method section) showing air temperature for four different time-slices: 50, 35, 20 and 10 Ma; respectively, for the early–middle Eocene, late Eocene to Oligocene, early Miocene, and middle–late Miocene records of Stereogenyini, plus *Syriemys lelunensis* (white circle).

possible record of the group in the middle Eocene of Morocco (Aniny *et al.* 2022). The high surface temperatures of the Eocene, leading to high sealevels (Miller *et al.* 2020), would favour dispersion out of the Mediterranean realm by that epoch. However, as summarized below, the fossil record of Stereogenyini suggests that such events happened somewhat later.

From that starting point, a palaeobiogeographical model (Fig. 8) could be drawn in which the Mediterranean Tethys offered an open connection to both the Atlantic and Indian oceans, the latter opening lasting at least until the Oligocene (Palcu & Krijgsman 2022). This enabled the ancestors of *Br. gaffneyi* to disperse to the Indo-Tethys, and those of '*Ba.*' *healeyorum* to reach the

North Atlantic western margin. However, because our phylogenetic hypothesis (Fig. 7) does not show *Br. gaffneyi* forming a clade with *Pi. auffenbergi* and *Sh. pilgrimi*, it is possible that some kind of Mediterranean–Indian connection remained open until the Miocene, enabling the dispersal of the ancestors of those two taxa by that epoch. Instead, if the connection did not last until then, but also following our phylogenetic hypothesis, the *Pi. auffenbergi* plus *Sh. pilgrimi* lineage could have reached the Indo-Tethys by the Oligocene, remaining unrecorded until the next epoch. Another possibility, not supported by the current phylogenetic results, is that all Indian Ocean Stereogenyini are closely related, representing a lineage that further diversified during the Miocene, following an Oligocene dispersion from the Mediterranean area.

A similar scenario can be drawn for the Caribbean record of Stereogenyini, although the Mediterranean–Atlantic connection was probably not closed for a significant amount of time prior to the Messinian Salinity Crisis (de la Vara *et al.* 2015). Given that our phylogenetic hypothesis (Fig. 7) does not show '*Ba.*' *healeyorum* close to the Miocene *Ba.* spp. clade, these two taxa either represent a double Oligocene dispersal event, with the *Ba.* spp. lineage remaining unrecorded until the next epoch, or *Ba.* spp. corresponds to a Miocene dispersal. Alternatively, but equally not supported by the current phylogenetic results, the Atlantic Stereogenyini could be closely related to one another, representing a lineage that diversified during the Miocene, following an Oligocene dispersion from the Mediterranean.

CONCLUSION

Syriemys lelunensis is the only definitive Stereogenyini turtle reported from the Arabian Platform, with possible occurrences in the Miocene of Oman and Saudi Arabia, and in the Oligocene of Oman. Previously, the oldest Stereogenyini were from the upper Eocene of Egypt, therefore our discovery extends the origin of the group by more than 10 myr, reinforcing its Mediterranean ancestral geographical range. Several palaeobiogeographical scenarios can explain the distribution of the marine or coastal Stereogenyini along the tropical seas of the northern hemisphere during the Cenozoic, but our phylogenetic analysis, similar to that provided by Ferreira *et al.* (2018a), precludes single dispersion events from the Mediterranean area to the Atlantic and Indian oceans.

Acknowledgements. This work is dedicated to geologists Mayson Al-Bitar and Rowaida Helou, two inspiring women scientists whose contributions to micropalaeontological research strengthened the foundation of geological and palaeontological studies in Syria. Their dedication and expertise played a vital role in advancing the understanding of Syrian microfossils, setting an example for future Syrian women in science. We are thankful to all of the individuals who played an important role in supporting and facilitating our work in Syria. Special thanks are due to the dedicated personnel at the General Establishment for Geology and Mineral Resources in Aleppo, including Mohammad Ibrahim, Ali Abdallah and Hasan Sadeq; and in Damascus, including the previous general manager Dr Mazhar Ibrahim, and the working team including Dorgham Diab, Evlin Khadour, Mohammad Alhasan, Bushra Shehab, Mohammad Merhej, Marwan Kherbek and Magdalen Shaheen. We also express our appreciation to Eng. Farah Mouty for facilitating communication with Daffodil 88 Medical Centre. Our thanks go to the management and team members of the centre for their invaluable support, including Dr Nedal Daoud, Dr Aladdin Daoud, Dr Maher Salamon, Abdullah Daoud, Issa Asami, Rima Al-Jarrah, Eng. Mohammed Najm, Wissam Duha, Natasha Ali, Mosaab Haj Hussein, Amir Abdullah and Iman Al-Saleh. Finally, we are grateful for the assistance of Dr Musadak Khatib, Ahmad Khaled, Roj Mousa, Ibrahim Murad, Obaida Sayed Ali and Marcel Lacerda. This research was funded by the São Paulo Research Foundation (FAPESP grant number 20/07997-4 to MCL). Many thanks also to the referees, Juliana Sterli and one anonymous reviewer, the Editor-in-Chief Michael Benton, the Editor Laura Porro and the Publications Officer Sally Thomas for their constructive comments that allowed us to improve our manuscript.

Author contributions. **Conceptualization** W.A. Alhalabi (WAAH), M.C. Langer (MCL), D.J. Martucci Neto (DJMN), G.S. Ferreira (GSF); **Data Curation** WAAH, MCL, GSF; **Formal Analysis** WAAH, MCL, DJMN, GSF; J. Ayoub (JA), E.A.M. Koutsoukos, (EAMK); **Funding Acquisition** MCL; **Investigation** WAAH, MCL, DJMN, GSF, JA, EAMK, I. Bou Jaoude (IBJ), H.M. Naser (HMN), J. Ayoub (JA), L. Abboud (LA), R. Shati (RS); **Methodology** WAAH, MCL, DJMN, GSF; **Project Administration** WAAH, MCL; **Resources** WAAH, MCL, GSF; **Software** MCL, GSF, DJMN; **Supervision** WAAH, MCL; **Validation** WAAH, MCL, DJMN, GSF; **Visualization** MCL, DJMN, GSF, IBJ; **Writing – Original Draft Preparation** WAAH, MCL, DJMN, GSF, IBJ, JA, RS; **Writing – Review & Editing** WAAH, MCL, DJMN, GSF, IBJ, EAMK.

DATA ARCHIVING STATEMENT

Phylogenetic data (matrix and character list) are available in MorphoBank (http://morphobank.org/permalink/?P5957). CT scan data for specimen GEGMRD 0002 (*Syriemys leluensis*) can be accessed via MorphoSource: https://doi.org/10.17602/M2/M754417 (volumetric image series); https://doi.org/10.17602/M2/M754501 (right pelvic bones, mesh); https://doi.org/10.17602/M2/M754497 (left pelvic bones, mesh); https://doi.org/10.17602/M2/M754421 (left femur, mesh).

This published work and the nomenclatural acts it contains, have been registered in ZooBank:

https://zoobank.org/References/EE498630-D0C3-4FBF-83DC-DC793208084C

Editor. Laura Porro

SUPPORTING INFORMATION

Additional Supporting Information can be found online (https://doi.org/10.1002/spp2.70026):

Appendix S1. Nexus file.
Appendix S2. Changes to the phylogenetic matrix.

REFERENCES

Alhalabi, W. A., Bardet, N., Sachs, S., Kear, B. P., Joude, I. B., Yazbek, M. K., Godoy, P. L. and Langer, M. C. 2024. Recovering lost time in Syria: new Late Cretaceous (Coniacian–Santonian) elasmosaurid remains from the Palmyrides mountain chain. *Cretaceous Research*, **159**, 105871.

Alhalabi, W. A., Martucci Neto, D. J., Ferreira, G. S., Bou Jaoude, I., Naser, H. M., Ayoub, J., Abboud, L., Shati, R., Koutsoukos, E. A. M. and Langer, M. C. 2025. Project 5957: Recovering lost time in Syria: a new Eocene Stereogenyini turtle from the Aleppo Plateau [dataset]. MorphoBank. http://morphobank.org/permalink/?P5957

Al Maleh, A. K. and Bardet, N. 2003. Découverte de niveaux phosphatés associés à des restes de vertébrés dans les dépôts carbonatés du Coniacien–Santonien du Jabal Abtar: épisode précoce de la phosphatogenèse sénonienne des Palmyrides (Syrie centrale). *Comptes Rendus, Géoscience*, **335**, 391–400.

Andrews, C. W. 1901. Preliminary note on some recently discovered extinct vertebrates from Egypt (Part II). *Geological Magazine (New Series, Decade IV)*, **8**, 436–444.

Andrews, C. W. 1903. On some pleurodiran chelonians from the Eocene of the Fayum, Egypt. *Annals and Magazine of Natural History Series 7*, **11** (61), 115–122.

Aniny, F., Bourdon, E., Adnet, S., Jouve, S., Zair, H., Gingerich, P. D., Elboudali, N. and Zouhri, S. 2022. The oldest Eocene marine vertebrate fauna from the Sahara Desert in southwestern Morocco. 3–5. *In* Çiner, A., Naitza, S., Radwan, A. E., Hamimi, Z., Lucci, F., Knight, J., Cucciniello, C., Banerjee, S., Chennaoui, H., Doronzo, D. M., Candeias, C., Rodrigo-Comino, J., Kalatehjari, R., Shah, A. A., Gentilucci, M., Panagoulia, D., Chaminé, H. I., Barbieri, M. and Ergüler, Z. A. (eds) *Recent research on sedimentology, stratigraphy, paleontology, geochemistry, volcanology, tectonics, and petroleum geology: MedGU 2022*. Springer. Advances in Science, Technology & Innovation.

Barakat, M. 2006. Mount Lelun in the Mirror of History. Ministry of Information in Damascus, Syria, No. 91641 (27 April).

Bardet, N., Cappetta, H., Suberbiola, X. P., Mouty, M., Al Maleh, A. K., Ahmad, A. M., Khrata, O. and Gannoum, N. 2000. The marine vertebrate faunas from the Late Cretaceous phosphates of Syria. *Geological Magazine*, **137**, 269–290.

Berggren, W. A. and Pearson, P. N. 2005. A revised tropical to subtropical Paleogene planktonic foraminiferal zonation. *The Journal of Foraminiferal Research*, **35**, 279–298.

Berggren, W. A., Kent, D. V., Swisher, C. C. III and Aubry, M.-P. 1995. A revised Cenozoic geochronology and chronostratigraphy. 129–212. *In* Berggren, W. A., Kent, D. V., Aubry, M.-P. and Hardenbol, J. (eds) *Geochronology, time scales and global stratigraphic correlation*. SEPM (Society for Sedimentary Geology) Special Publication 54.

Brew, G., Barazangi, M., Al-Maleh, A. K. and Sawaf, T. 2002. Tectonic and geologic evolution of Syria. *GeoArabia*, **6**, 573–616.

Cadena, E. A., Scheyer, T. M., Carrillo-Briceño, J. D., Sánchez, R., Aguilera-Socorro, O. A., Vanegas, A., Pardo, M., Hansen, D. M. and Sánchez-Villagra, M. R. 2020. The anatomy, paleobiology, and evolutionary relationships of the largest extinct side-necked turtle. *Science Advances*, **6** (7), eaay4593.

Cadena, E. A., Link, A., Cooke, S. B., Stroik, L. K., Vanegas, A. F. and Tallman, M. 2021. New insights into the anatomy and ontogeny of the largest extinct freshwater turtles. *Heliyon*, **7** (12), e08591.

Cherney, M. D., Wilson Mantilla, J. A., Gingerich, P. D., Zalmout, I. and Antar, M. S. M. 2020. New specimens of the late Eocene turtle *Cordichelys* (Pleurodira: Podocnemididae) from Wadi Al Hitan and Qasr El-Sagha in the Fayum Province of Egypt. *Contributions from the Museum of Palaeontology, University of Michigan*, **33** (2), 29–64.

Cohen, K. M., Finney, S. C., Gibbard, P. L. and Fan, J. X. 2013. The ICS international chronostratigraphic chart. *Episodes*, **36**, 199–204.

Cope, E. D. 1865. Third contribution to the herpetology of tropical America. *Proceedings of the Academy of Natural Sciences of Philadelphia*, **17**, 185–198.

Cope, E. D. 1868. On the origin of genera. *Proceedings of the Academy of Natural Sciences of Philadelphia*, **20**, 242–300.

Dacqué, E. 1912. Die fossilen Schildkröten Aegyptens. *Geologische und Palaeontologische Abhandlungen (n.s.)*, **14**, 275–337.

de Broin, F. 1977. Contribution à l'étude des Chéloniens: Chéloniens continentaux du Crétacé et du Tertiaire de France. *Mémoires du Muséum National d'Histoire Naturelle, Nouvelle Série*, **38**, 1–366.

de Broin, F. 1988. Les tortues et le Gondwana. Examen des rapports entre le fractionnement du Gondwana et la dispersion géographique des tortues pleurodires à partir du Crétacé. 103–142. *In* Jiménez-Fuentes, E. and de Broin, F. (eds) *Studia Palaeocheloniologica. Vol. 2*. Ediciones Universidad de Salamanca.

de la Vara, A., Topper, R. P., Meijer, P. T. and Kouwenhoven, T. J. 2015. Water exchange through the Betic and Rifian corridors prior to the Messinian Salinity Crisis: a model study. *Paleoceanography*, **30**, 548–557.

Ferreira, G. S., Rincon, A. D., Solorzano, A. and Langer, M. C. 2015. The last marine pelomedusoids (Testudines: Pleurodira): a new species of *Bairdemys* and the paleoecology of Stereogenyina. *PeerJ*, **3**, e1063.

Ferreira, G. S., Bandyopadhyay, S. and Joyce, W. G. 2018a. A taxonomic reassessment of *Piramys auffenbergi*, a neglected

turtle from the late Miocene of Piram Island, Gujarat, India. *PeerJ*, **6**, e5938.

Ferreira, G. S., Bronzati, M., Langer, M. C. and Sterli, J. 2018b. Phylogeny, biogeography and diversification patterns of side-necked turtles (Testudines: Pleurodira). *Royal Society Open Science*, **5** (3), 171773.

Ferreira, G. S., Nascimento, E. R., Cadena, E. A., Cozzuol, M. A., Farina, B. M., Pacheco, M. L. A. F., Rizzutto, M. A. and Langer, M. C. 2024. The latest freshwater giants: a new *Peltocephalus* (Pleurodira: Podocnemididae) turtle from the Late Pleistocene of the Brazilian Amazon. *Biology Letters*, **20** (3), 20240010.

Gaffney, E. S. and Wood, R. C. 2002. *Bairdemys*, a new side-necked turtle (Pelomedusoides: Podocnemididae) from the Miocene of the Caribbean. *American Museum Novitates*, **3359**, 1–28.

Gaffney, E. S., Scheyer, T. M., Johnson, K. G., Bocquentin, J. and Aguilera, O. A. 2008. Two new species of the side necked turtle genus, *Bairdemys* (Pleurodira, Podocnemididae), from the Miocene of Venezuela. *Palaeontologische Zeitzschrift*, **82**, 209–229.

Gaffney, E. S., Meylan, P. A., Wood, R. C., Simons, E. and Campos, D. D. A. 2011. Evolution of the side-necked turtles: the family Podocnemididae. *Bulletin of the American Museum of Natural History*, **2011** (350), 1–237.

Hijmans, R. 2025. terra: spatial data analysis. R package version 1.8-25, https://rspatial.github.io/terra/, https://rspatial.org/

Hutchison, J. H. and Bramble, D. M. 1981. Homology of the plastral scales of the Kinosternidae and related turtles. *Herpetologica*, **37**, 73–85.

ICVGAN. 2005. *Nomina anatomica veterinaria*, Fifth edition. International Committee on Veterinary Gross Anatomical Nomenclature.

Kampouridis, P., Hartung, J. and Augustin, F. J. 2023. The Eocene–Oligocene vertebrate assemblages of the Fayum Depression, Egypt. 373–405. *In* Hamimi, Z., Khozyem, H., Adatte, T., Nader, F. H., Oboh-Ikuenobe, F., Zobaa, M. K. and El Atfy, H. (eds) *The Phanerozoic geology and natural resources of Egypt*. Springer. Advances in Science, Technology & Innovation. https://doi.org/10.1007/978-3-030-95637-0_14

Kocsis, Á. T. and Scotese, C. R. 2021. Mapping paleocoastlines and continental flooding during the Phanerozoic. *Earth-Science Reviews*, **213**, 103463.

Kocsis, Á. T., Raja, N. B., Williams, S. and Dowding, E. M. 2024. rgplates: R interface for the GPlates web service and desktop application. https://zenodo.org/doi/10.5281/zenodo.8093990

Miller, K. G., Browning, J. V., Schmelz, W. J., Kopp, R. E., Mountain, G. S. and Wright, J. D. 2020. Cenozoic sea-level and cryospheric evolution from deep-sea geochemical and continental margin records. *Science Advances*, **6**, aaz1346.

Müller, R. D., Cannon, J., Qin, X., Watson, R. J., Gurnis, M., Williams, S., Pfaffelmoser, T., Seton, M., Russell, S. H. J. and Zahirovic, S. 2018. GPlates: building a virtual Earth through deep time. *Geochemistry, Geophysics, Geosystems*, **19**, 2243–2261.

Palcu, D. V. and Krijgsman, W. 2022. The dire straits of Paratethys: gateways to the anoxic giant of Eurasia. *Geological Society, London, Special Publications*, **523**, 111–139.

Pebesma, E. 2018. Simple features for R: standardized support for spatial vector data. *The R Journal*, **10**, 439–446.

Pebesma, E. and Bivand, R. 2023. *Spatial data science: With applications in R*. Chapman & Hall/CRC. https://doi.org/10.1201/9780429459016

Pérez-García, A., De Broin, F. d. L. and Murelaga, X. 2017. The *Erymnochelys* group of turtles (Pleurodira, Podocnemididae) in the Eocene of Europe: new taxa and paleobiogeographical implications. *Palaeontologia Electronica*, **20** (1), 14A.

Pérez-García, A., Guerrero, A., Martín de Jesús, S. and Ortega, F. 2024. Shell anatomy and intraspecific variability of the Spanish Lutetian podocnemidid turtle *Neochelys zamorensis*. *Palaeontologia Electronica*, **27** (2), a28.

Pérez-García, A., Guerrero, A., Martín de Jesús, S. and Ortega, F. 2025. Shell characterization of the youngest valid species of the European Eocene genus *Neochelys* (Pleurodira, Podocnemididae): the Spanish Bartonian *Neochelys salmanticensis*. *The Anatomical Record*, **308**, 1553–1572.

Prasad, K. N. 1974. The vertebrate fauna from Piram Island, Gujarat, India. *Memoires of the Geological Survey of India, New Series*, **41**, 1–23.

Protasevich, L., Maximov, A. and Tkachev, G. 1963. Geological map of Syria. Sheet J-37-I & II. Syrian Arab Republic, Ministry of Industry, Department of Geological and Mineral Research.

Protasevich, L. N., Maksimov, A. A., Ponikarov, V. P. and Pavlov, F. V. 1966. The geological map of Syria, Sheet J-37-I & II-Explanatory Notes. Syrian Arab Republic, Ministry of Industry, Department of Geological and Mineral Research.

R Core Team. 2024. R: a language and environment for statistical computing. R Foundation for Statistical Computing, Vienna, Austria. https://www.R-project.org/

Roger, J., Pickford, M., Thomas, H., De Broin, F. D. L., Tassy, P., Van Neer, W., Bourdillon-De-Grissac, C. and Al-Busaldi, S. 1994. Découverte de vertébrés fossiles dans le Miocène de la région du Huqf au Sultanat d'Oman. *Annales de Paléontologie*, **80**, 253–273.

Romer, A. S. 1956. *Osteology of the reptiles*. University of Chicago Press, 772 pp.

Rukieh, M., Trifonov, V. G., Dodonov, A. E., Minini, H., Ammar, O., Ivanova, T. P., Zaza, T., Yusef, A., Al-Shara, M. and Jobaili, Y. 2005. Neotectonic map of Syria and some aspects of Late Cenozoic evolution of the northwestern boundary zone of the Arabian plate. *Journal of Geodynamics*, **40**, 235–256.

Savioz, N. R. and Morel, P. 2005. La faune de Nadaouiyeh Aïn Askar (Syrie centrale, Pléistocène moyen): aperçu et perspectives. *Revue de Paléobiologie, Genève*, **10**, 31–35.

Scotese, C. R., Song, H., Mills, B. J. and van der Meer, D. G. 2021. Phanerozoic paleotemperatures: the earth's changing climate during the last 540 million years. *Earth-Science Reviews*, **215**, 103503.

Swinton, W. E. 1939. A new fresh-water tortoise from Burma. *Records of the Geological Survey of India*, **74**, 548–551.

Thomas, H. 1982. The Lower Miocene fauna of Al-Sarrar (Eastern Province, Saudi Arabia). *ATLAL: The Journal of Saudi Arabian Archaeology*, **5**, 109–136.

Thomas, H., Roger, J., Sen, S., Bourdillon-De-Grissac, C. and Al-Sulaimani, Z. 1989. Découverte de Vertébrés fossiles dans l'Oligocène inférieurdu Dhofar (Sultanat d'Oman). *Geobios*, **22**, 101–120.

Valdes, P. J., Scotese, C. R. and Lunt, D. J. 2021. Deep ocean temperatures through time. *Climate of the Past*, **17**, 1483–1506.

Weems, R. E. and Knight, J. L. 2013. A new species of *Bairdemys* (Pelomedusoides: Podocnemididae) from the Oligocene (Early Chattian) Chandler Bridge Formation of South Carolina, USA, and its paleobiogeographic implications for the genus. Morphology and evolution of turtles. 289–303. *In* Brinkman, D., Holroyd, P. and Gardner, J. (eds) *Morphology and evolution of turtles*. Springer. Vertebrate Paleobiology and Paleoanthropology.

Wood, R. C. 1970. A review of the fossil Pelomedusidae (Testudines, Pleurodira) of Asia. *Breviora*, **357**, 1–24.

Wood, R. C. and Díaz de Gamero, M. L. D. 1971. *Podocnemis venezuelensis*, a new fossil pelomedusid (Testudines, Pleurodira) from the Pliocene of Venezuela and a review of the history of *Podocnemis* in South America. *Breviora*, **376**, 1–23.